



Design and synthesis of novel macrocyclic 2-amino-6-arylpyrimidine Hsp90 inhibitors

Atsushi Suda*, Hiroshi Koyano, Tadakatsu Hayase, Kihito Hada, Ken-ichi Kawasaki, Susumu Komiyama, Kiyoshi Hasegawa, Takaaki A. Fukami, Shigeo Sato, Takaaki Miura, Naomi Ono, Toshikazu Yamazaki, Ryoichi Saitoh, Nobuo Shimma, Yasuhiko Shiratori, Takuo Tsukuda

Kamakura Laboratories, Research Division, Chugai Pharmaceutical Co., Ltd, 200 Kajiwara, Kamakura, Kanagawa 247-8530, Japan

ARTICLE INFO

Article history:

Received 11 October 2011
Revised 17 November 2011
Accepted 24 November 2011
Available online 1 December 2011

Keywords:

Structure-based drug design
Lead optimization
Macrocyclic molecule
Antitumor agent
Hsp90 inhibitor

ABSTRACT

Macrocyclic compounds bearing a 2-amino-6-arylpyrimidine moiety were identified as potent heat shock protein 90 (Hsp90) inhibitors by modification of 2-amino-6-aryltriazine derivative (CH5015765). We employed a macrocyclic structure as a skeleton of new inhibitors to mimic the geldanamycin-Hsp90 interactions. Among the identified inhibitors, CH5164840 showed high binding affinity for N-terminal Hsp90 α ($K_d = 0.52$ nM) and strong anti-proliferative activity against human cancer cell lines (HCT116 $IC_{50} = 0.15$ μ M, NCI-N87 $IC_{50} = 0.066$ μ M). CH5164840 displayed high oral bioavailability in mice ($F = 70.8\%$) and potent antitumor efficacy in a HCT116 human colorectal cancer xenograft model (tumor growth inhibition = 83%).

© 2011 Elsevier Ltd. All rights reserved.

Heat shock protein 90 (Hsp90) is an ATP-dependent molecular chaperon which is constitutively and ubiquitously expressed in mammalian cells. It governs the conformational maturation, stability and function of these substrate proteins, called client proteins.¹ Because client proteins are known to play an important role in controlling proliferation, survival, invasion, metastasis, and angiogenesis, Hsp90 inhibitors could cause potent inhibition of tumor growth and progression by simultaneous degradation of client proteins.^{2–4} Indeed, it has been reported that the ansamycin antibiotic geldanamycin (GM, **1a**)⁵ and the macrocyclic lactone antibiotic radicicol (RD, **2**)⁶ demonstrated anti-proliferative activity against tumor cells by inhibiting Hsp90 (Fig. 1). The selective effect of these inhibitors to tumor cells and not to normal cells might stem from the fact that Hsp90 exists in an activated state in tumor cells by forming a complex with a series of co-chaperones.^{7–10} Consequently, Hsp90 is believed to be an attractive molecular target for anticancer agents.^{2–4} Actually, several Hsp90 inhibitors such as semi-synthetic analogs of GM, 17-allylamino-17-demethoxygeldanamycin (17-AAG, **1b**)¹¹ and 17-(2-dimethylaminoethylamino)-17-demethoxygeldanamycin (17-DMAG, **1c**)¹² along with synthetic small molecules such as CNF-2024 (**3**),¹³ NVP-AUY922 (**4**)¹⁴ and AT13387 (**5**)¹⁵ are being evaluated in clinical trials (Fig. 1).

We recently reported the identification of a new class of orally available Hsp90 inhibitor bound to the N-terminal ATP binding site, CH5015765 (**6**), by a combination of fragment screening, virtual screening, and structure-based drug design with the assistance of X-ray cocrystal structures of ligand-Hsp90 complexes.¹⁶

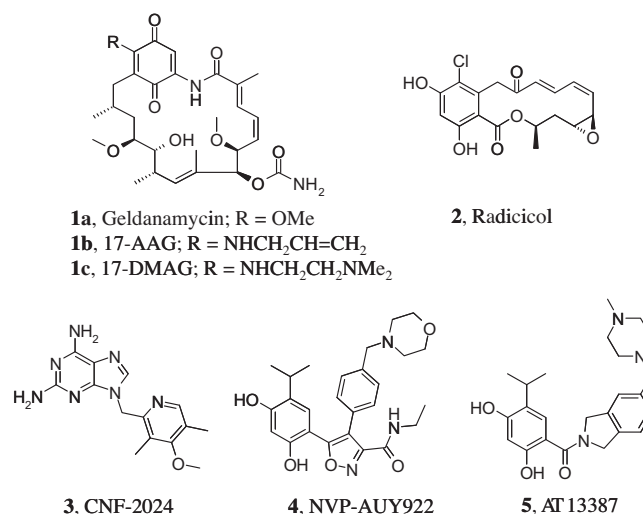


Figure 1. Known Hsp90 inhibitors.

* Corresponding author. Tel.: +81 467 47 6067; fax: +81 467 45 6824.

E-mail address: sudaats@chugai-pharm.co.jp (A. Suda).

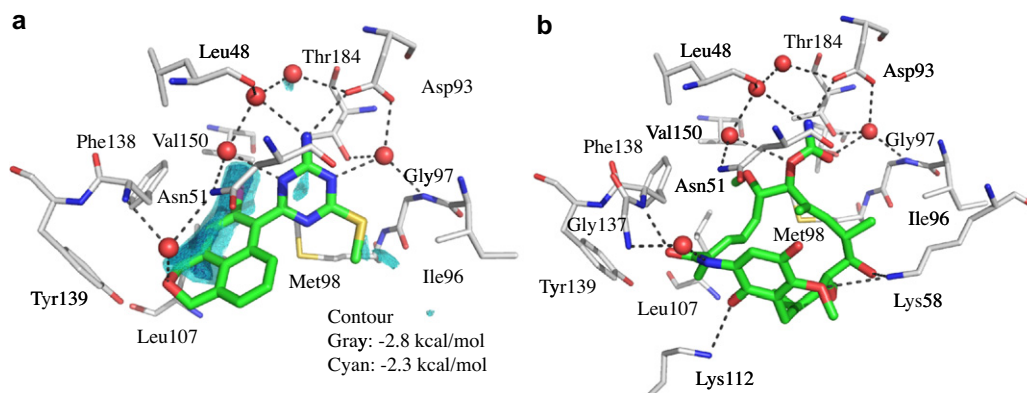
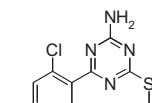


Figure 2. X-ray structure analysis of small molecular Hsp90 inhibitors in complex with human N-terminal Hsp90α. The numbering of the residues corresponds to those in the X-ray cocrystal structure (gray C_{Hsp90α}, green C_{ligand}, red O, blue N, yellow S, purple Cl). Hydrogen bonds are indicated by dashes. (a) Detailed binding mode of compound **6** (PDB code: 3B28). Hydrophobic space was predicted by the Site Finder application in MOE and its location is shown in cyan (-2.3 kcal/mol) and gray (-2.8 kcal/mol). (b) Detailed binding mode of GM (PDB code: 1YET).

Table 1
Chemical structure of **6** and its biological,¹⁶ physicochemical, and pharmacokinetic profiles



6, CH5015765

(a) Binding affinity, in vitro anti-proliferative activity, and physicochemical properties of **6**

K_d (nM) ^a	IC ₅₀ (μM)		PSA (Å ²) ^b	Solubility (μM) ^c	LM CL (μL/min/mg protein)	
	HCT116	NCI-N87			Human	Mouse
3.4	0.46	0.57	59.1	29	43	60

(b) Pharmacokinetic profiles of **6**

Administration	Dose (mg/kg)	$t_{1/2}$ (h)	t_{max} (h)	C_{max} (μg/mL)	AUC _{inf} (μg·h/mL)	CL or CL/F (mL/h/kg)	F^d (%)
iv	10	0.25	—	—	8.55	1170	—
po	200	2.62	0.5	3.92	7.65	26100	4.5

^a Values were measured by surface plasmon resonance (SPR) using human N-terminal Hsp90α.

^b Molecular polar surface area (PSA) was calculated by TPSA.

^c Solubility in FaSSIF. The use of FaSSIF may over-predict the solubility in physiological in vivo conditions.

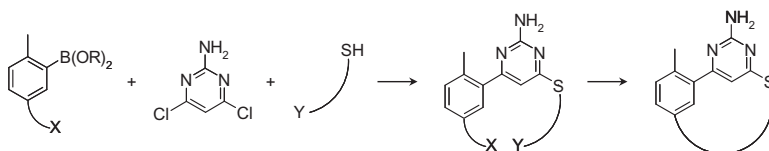
^d Oral bioavailability.

Compound **6** showed high affinity for N-terminal Hsp90 ($K_d = 3.4$ nM) and in vitro anti-proliferative activity against cell lines such as KRAS mutant HCT116 (IC₅₀ = 0.46 μM) and HER2-overexpressing NCI-N87 (IC₅₀ = 0.57 μM). In mice, however, it showed several drawbacks such as limited oral bioavailability ($F = 4.5\%$) and moderate tumor growth inhibition (TGI = 54%) against the xenografted NCI-N87 (po, 400 mg/kg). These drawbacks probably came from the low liver microsomal (LM) stability (mouse LM clearance (CL) = 60 μL/min/mg protein) and low water solubility (solubility in fasted state simulated intestinal fluid (FaSSIF) = 29 μM). In this work, compound **6** was chosen as a lead compound for further optimization, and biological,¹⁶ physicochemical, and pharmacokinetic profiles of **6** are summarized in Table 1.

In an X-ray cocrystal structure of **6** with human Hsp90 (PDB code: 3B28), we observed the following effective interactions, as depicted in Figure 2a: (1) an amino group on the 2-position of triazine forms multiple hydrogen bonds with the carboxylic side chain of Asp93 and a water molecule which is conserved in the cocrystal structures of all Hsp90 ATP site binders; (2) a methylthio group on the 4-position of triazine forms a hydrophobic interaction

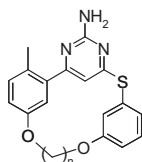
with hydrophobic side chains of Ile96 and Met98; (3) a hydrophobic part from the chloro group to benzylic methylene carbon of a 5-chloro-1H,3H-benzo[de]isochromene moiety fills the proximal hydrophobic space formed by hydrophobic side chains of Val150, Leu107, and Phe138 (explicitly visualized by the Site Finder application in Molecular Operating Environment¹⁷); (4) an etheric oxygen of a 5-chloro-1H,3H-benzo[de]isochromene moiety forms a hydrogen bond with a water molecule which is hydrogen-bonded to the backbone of Phe138 and the side chain of Asn51. On the other hand, we analyzed the binding mode of GM (PDB code: 1YET) and identified important interactions such as one with the side chain of Lys58 (Fig. 2b).¹⁶ In our molecular design of new inhibitors, we maintained the interactions found between compound **6**-Hsp90 and tried to incorporate GM-Hsp90 interactions.

We considered that a macrocyclic structure like GM would offer more chances to make effective interactions. In general, macrocyclic compounds are more conformationally restricted than their acyclic analogs, which potentially give higher target bindings and selectivities and improve oral bioavailabilities.^{18,19} We chose pyrimidine instead of triazine as a core structure since a nitrogen



Scheme 1. Synthetic route of macrocyclic derivatives.

Table 2
Binding affinity and in vitro anti-proliferative activity of ether linkage derivatives



Compd	n	Ring size	K _d ^a (nM)	IC ₅₀ (μM)	
				HCT116	NCI-N87
7	3	15	120	10.3	11.3
8	4	16	40	5.5	3.8
9	5	17	84	3.7	2.9

^a Values were measured by SPR using human N-terminal Hsp90α.

atom at the 5-position of **6** does not interact with the protein. In addition, an *o*-tolyl moiety was employed instead of a 5-chloro-1*H*,3*H*-benzo[*de*]isochromene moiety as a minimum structural requirement for the necessary hydrophobic interactions. The selection of these moieties enables the general synthetic route depicted in **Scheme 1**. Thus, Suzuki–Miyaura cross-coupling of the *o*-tolyl moiety bearing an appropriate functional group (X) to pyrimidine core and nucleophilic introduction of a sulfanyl moiety bearing a counterpart (Y) followed by cyclization with X and Y gives macrocyclic derivatives.

First, we designed and synthesized **7**, **8** and **9** as prototypes of macrocyclic derivatives. A phenyl group was connected to sulfur atom at the 4-position of the core structure to increase a hydrophobic interaction to Ile96 and Met98. The two phenyl groups were linked by 3, 4 and 5 of methylene carbons via etheric oxygen atoms. The binding affinities and in vitro anti-proliferative activities of these derivatives are summarized in **Table 2**. The binding affinity of **8** was the highest in the three compounds, but it was ten times weaker than that of **6** (**Table 1**). An X-ray cocrystal structure of **8** and Hsp90 (PDB code: 3VHA, 1.4 Å resolution) revealed that the etheric oxygen at the 5'-position of a phenyl ring did not form the hydrogen bond ($d(O\cdots O_{\text{water}}) = 3.9 \text{ \AA}$) with the water molecule which itself forms hydrogen bonds with the backbone of Phe138 and the side chain of Asn51, although a carbon atom at the 1'-position of a phenyl ring formed aryl–alkyl interactions ($d(C\cdots C_{\text{Ile96}}) = 4.1 \text{ \AA}$) with the 3-methyl group of Ile96 and ($d(C\cdots C_{\text{Met98}}) = 3.9 \text{ \AA}$) with the 4-methylene group of Met98 (**Fig. 3a**). (For a detailed discussion of noncovalent interactions, see Bissantz et al.)²⁰

Following this, a 2',4'-disubstitued derivative was designed in order to achieve enhanced hydrophobic interactions by further occupation of the hydrophobic space formed by Val150, Leu107, and Phe138. As expected, 2',4'-dichloro derivative **10** showed about four times stronger binding affinity than **8**. A 2',4'-dimethyl-5'-benzamide derivative **11**, with a K_d value of 1.3 nM, achieved both the hydrophobic interaction and the hydrogen bond formation with the water molecule which forms hydrogen bonds

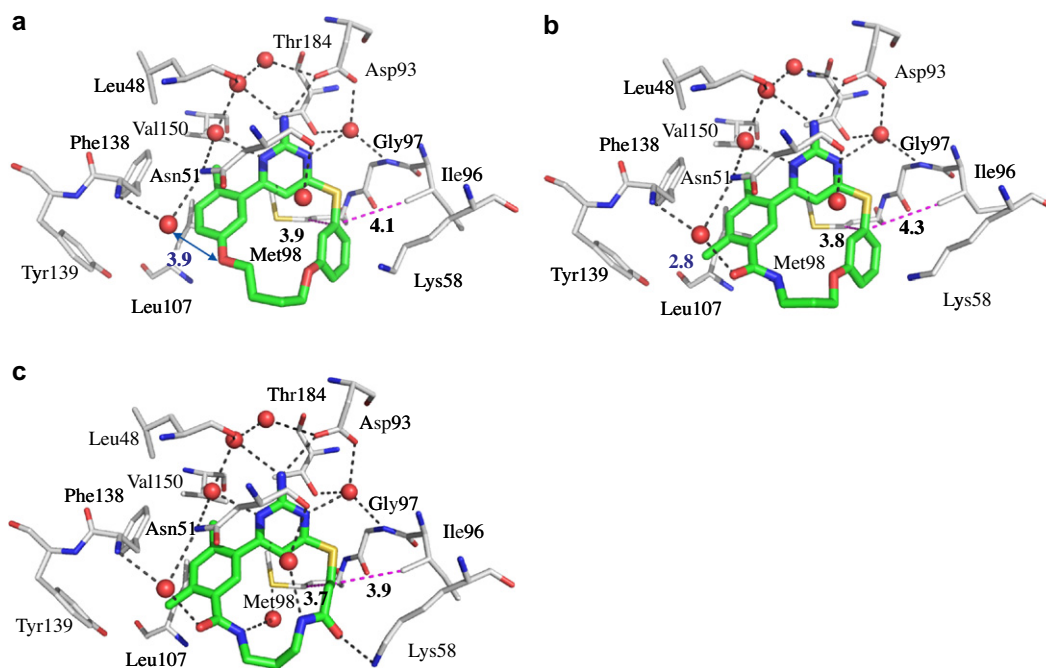
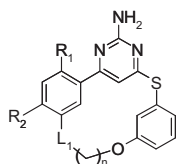


Figure 3. X-ray structures of N-terminal Hsp90α in complex with identified compounds. The numbering of the residues corresponds to those in the X-ray cocrystal structure (gray C_{Hsp90α}, green C_{ligand}, red O, blue N, yellow S). Distances are given in Å. Noncovalent interactions are indicated by dashes (black: hydrogen bonds, magenta: hydrophobic interactions). Detailed binding modes of (a) compound **8** (PDB code: 3VHA), (b) compound **11** (PDB code: 3VHC), (c) compound **16** (PDB code: 3VHD).

Table 3

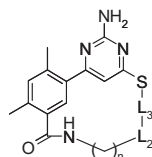
Binding affinity, in vitro anti-proliferative activity and water solubility of amide linkage derivatives having an aromatic side chain on the S atom



Compd	R ₁	R ₂	L ₁ ^a	n	Ring size	K _d (nM) ^b	IC ₅₀ (μM)		PSA (Å ²) ^c	Solubility (μM) ^d
							HCT116	NCI-N87		
8	Me	H	O	4	16	40	5.5	3.8	56.3	18
10	Cl	Cl	O	4	16	11	1.5	1.1	55.4	<7
11	Me	Me	-CONH-	3	16	1.3	0.78	0.94	71.0	79
12	Me	Me	-CONH-	4	17	7.4	2.5	3.3	71.1	69
13	Me	Me	-CONH-	5	18	6.2	3.1	3.0	72.1	39
14	Me	MeO	-CONH-	3	16	5.8	4.0	4.2	78.5	260
15	Me	EtO	-CONH-	3	16	10	4.1	4.3	78.3	186

^a Element order as seen left to right in a formula.^b Values were measured by SPR using human N-terminal Hsp90α.^c PSA was calculated by TPSA.^d Solubility in FaSSIF.**Table 4**

Binding affinity, in vitro anti-proliferative activity, and physicochemical properties of amide linkage derivatives having an aliphatic side chain on the S atom



Compd	n	L ₂ ^a	L ₃	Ring size	K _d (nM) ^b	IC ₅₀ (μM)			LM CL (μL/min/mg protein)	
						HCT116	NCI-N87	Solubility (μM) ^c	Human	Mouse
11	3	O	-1,3-C ₆ H ₄ -	16	1.3	0.78	0.94	79	56	93
16 , CH5164840	3	-NHCO-	-(CH ₂) ₂ -	16	0.52	0.15	0.066	125	0.28	2.3
17	4	-NHCO-	-(CH ₂) ₂ -	17	0.38	0.13	0.092	553	5.1	3.5
18	5	-NHCO-	-(CH ₂) ₂ -	18	0.25	0.21	0.091	169	1.7	1.8
19	2	-NHCO-	-(CH ₂) ₃ -	16	0.61	0.29	0.18	106	5.4	3.6
20	3	-CONH-	-(CH ₂) ₂ -	16	0.65	0.25	0.15	117	1	15
21	2	-OCONH-	-(CH ₂) ₂ -	16	0.7	0.13	0.1	911	3.5	7.3
22	2	-NHCOO-	-(CH ₂) ₂ -	16	0.8	0.13	0.17	111	9.3	21

^a Element order as seen left to right in a formula.^b The values were measured by SPR using human N-terminal Hsp90α.^c Solubility in FaSSIF.

with the backbone of Phe138 and the side chain of Asn51. The steric bulkiness of the methyl group of **11** is similar to that of the chloro group to achieve a hydrophobic interaction. This modification significantly improved the binding affinity and in vitro anti-proliferative activity (Table 3). An X-ray cocrystal structure of **11** and Hsp90 (PDB code: 3VHC, 1.4 Å resolution) revealed that the amide oxygen of **11** formed a hydrogen bond ($d(\text{O}\cdots\text{O}_{\text{water}}) = 2.8 \text{ \AA}$) with the water, which was not observed in **8**, and the 2'-dimethylphenyl group filled the hydrophobic space (Fig. 3b). In addition, **11** had better water solubility (solubility in FaSSIF = 79 μM) than the lead compound **6**, presumably due to increased molecular polar surface area (PSA, 71.0 Å² as calculated by TPSA^{21,22}). The ring size enlargement to 17- and 18-membered rings (**12** and **13**, respectively) by the addition of methylene carbons caused a reduction in binding affinity (Table 3). These results indicate that 16-membered ring is also optimal in the case of the amide linkage derivatives. When we tried keeping the amide linkage and 16-membered ring and exchanging methyl to a methoxy or ethoxy group at the R₂ position (**14** and **15**, respectively), the water solubility was improved, but it led to a reduction in binding affinity

(Table 3). Therefore, R₂ group should be a small hydrophobic group such as a methyl or chloro group.

In an X-ray cocrystal structure of **11**-Hsp90, we observed a lack of the interaction of **11** to Lys58's side chain NH which is present in GM-Hsp90 complex (Fig. 3b). As a hydrogen bond acceptor, an alkylamide or a carbamate group (L₂) was introduced in between the amide nitrogen and sulfur (Table 4). Based on the molecular modeling analysis, we abandoned a phenylene group and used methylene carbons as L₃ to direct amide carbonyl oxygen toward Lys58. Hydrophobic interactions of methylene carbons with Ile96 and Met98 may contribute to affinity. As expected, an X-ray cocrystal structure of **16** and Hsp90 (PDB code: 3VHD, 1.3 Å resolution) revealed that the amide oxygen of **16** formed a hydrogen bond with the side chain of Lys58, and the methylene carbon attached to the S atom formed alkyl-alkyl interactions ($d(\text{C}\cdots\text{C}_{\text{Ile96}}) = 3.9 \text{ \AA}$) with Ile96 and ($d(\text{C}\cdots\text{C}_{\text{Met98}}) = 3.7 \text{ \AA}$) with Met98 (Fig. 3c). The alkylamide derivatives (**16**–**20**) showed improved binding affinities, in vitro anti-proliferative activity, solubility, and LM stability (Table 4). The carbamate derivatives also showed improvement in these profiles. Out of **16**–**22**, **16** showed the highest LM stability.

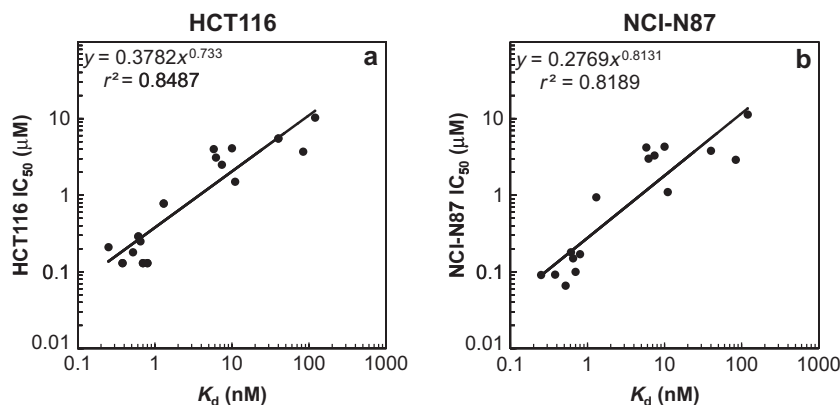


Figure 4. Correlation between K_d value (determined by SPR) and in vitro anti-proliferative activity (IC_{50}).

Table 5
PK parameters of **16** in nude mice

Administration	Dose (mg/kg)	$t_{1/2}$ (h)	t_{max} (h)	C_{max} ($\mu\text{g/mL}$)	AUC_{inf} ($\mu\text{g}\cdot\text{h/mL}$)	CL or CL/F (mL/h/kg)	F^a (%)
iv	3	1.66	—	—	9.07	337	—
po	3	2.64	0.5	2.93	6.42	468	70.8

^a Oral bioavailability.

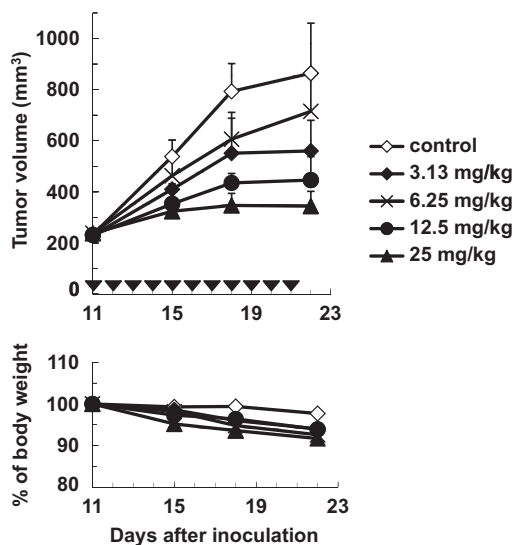


Figure 5. Growth inhibitory effect of **16** on HCT116 tumor xenograft model. SCID mice bearing HCT116 were administered compound **16** orally once daily for 11 consecutive days (days 11–21) at 3.13 mg/kg (TGI = 48%), 6.25 mg/kg (TGI = 25%), 12.5 mg/kg (TGI = 66%), and 25 mg/kg (TGI = 83%).

Human Hsp90 exhibits weak ATPase activity in the absence of co-chaperones.⁹ The conventional ATPase assay did not offer sufficient information for the lead optimization because of its inherent low sensitivity. Therefore, we used surface plasmon resonance (SPR) to assess inhibitor binding affinity. Positive correlation between K_d values and in vitro anti-proliferative activities (IC_{50}) against two cell lines was found for 16 derivatives (compounds **7–22**), which suggests that in vitro anti-proliferative activities were derived from inhibitory activities against Hsp90 (Fig. 4).

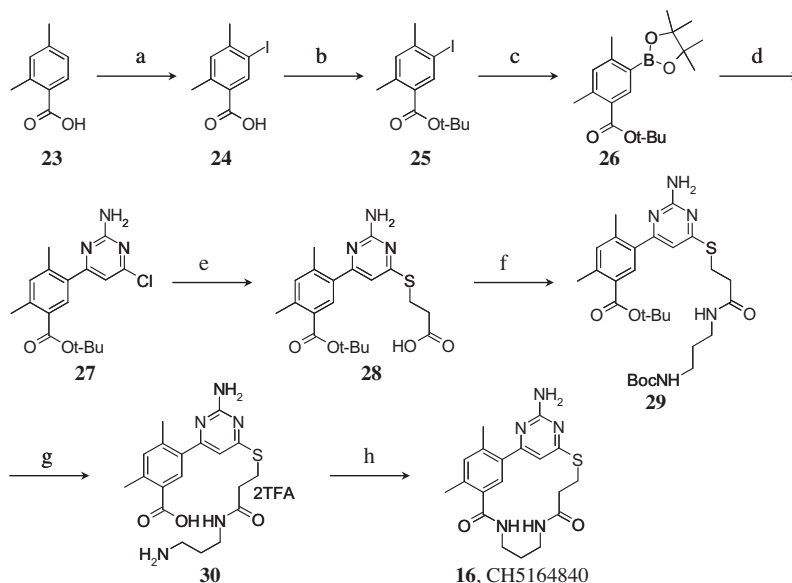
Since **16** showed high binding affinity, strong in vitro anti-proliferative activity, and sufficient in vitro metabolic stability, we conducted in vivo profiling. The pharmacokinetic study in mice demonstrated high oral bioavailability ($F = 70.8\%$) and favorable

plasma clearance, which is consistent with the low mouse LM clearance (Table 5).

Compound **16** was further evaluated in a human HCT116 colorectal cancer xenograft model in mice (Fig. 5). Mice bearing HCT116 were orally treated with **16** once daily for 11 days at 3.13, 6.25, 12.5, and 25 mg/kg, and their body weight and tumor volume were measured twice a week. Compound **16** showed potent antitumor efficacy with TGI of 83% without significant loss of body weight. In addition, **16** demonstrated potent antitumor efficacy especially in HER2-overexpressing cancer xenograft models when administered alone or in combination with the HER2-targeted agents such as trastuzumab and lapatinib.²³

The preparation of **16** is shown in Scheme 2. Boronate ester **26** was prepared from commercial 2,4-dimethylbenzoic acid (**23**) via selective iodination at the 4-position (75%), esterification (70%), and Miyaura borylation (94%). This boronate **26** was coupled with commercially available 2-amino-4,6-dichloropyrimidine by Pd-catalyzed Suzuki-Miyaura cross-coupling to give 2-amino-6-aryl-4-chloropyrimidine **27** (67%). Nucleophilic substitution with 3-mercaptopropionic acid gave **28** (75%) and following amide formation gave a Boc-protected precursor of macrocyclization **29** (71%). Deprotection followed by amide formation under highly diluted condition (2 mM) gave **16** (21% in 2 steps). A synthetic route amenable to scale-up preparation was established in our laboratories and the work is due to be reported in a separate publication.

In summary, we identified novel macrocyclic 2-amino-6-arylpyrimidines as Hsp90 inhibitors by modification of 2-amino-6-aryltriazine derivative (CH5015765). We employed a macrocyclic structure as a skeleton for the new inhibitors to mimic the GM-Hsp90 interactions and to improve the metabolic stability. This macrocyclic structure enabled us to introduce several functional groups, such as a carbonyl moiety at the appropriate position, with proper direction to interact with the key elements of the protein, resulting in significant improvement of the binding affinity together with antiproliferative activity. Among the macrocycles, compound **16** (CH5164840) showed low clearance and high solubility. The compound demonstrated high oral bioavailability in mice and potent antitumor efficacy in a human HCT116 colorectal cancer xenograft model.



Scheme 2. Synthesis of compound **16**^a. ^aReagents and conditions: (a) I₂, NaIO₄, Ac₂O, H₂SO₄, AcOH, 105 °C, 6 h, 75%; (b) *N,N*-dimethylformamide di-*tert*-butyl acetal, toluene, 80 °C, 2 h, 70%; (c) B₂pin₂, Pd₂Cl₂(dppf)-CH₂Cl₂, AcOK, DMF, 80 °C, 18 h, 94%; (d) 2-amino-4,6-dichloropyrimidine, Pd₂Cl₂(dppf)-CH₂Cl₂, NaHCO₃, 1,4-dioxane, H₂O, 80 °C, 19 h, 67%; (e) 3-mercaptopropionic acid, Cs₂CO₃, DMF, 80 °C, 2 h, 75%; (f) EDC-HCl, HOBT, *N*-Boc-1,3-propanediamine, DIPEA, DMF, rt, 6 h, 71%; (g) TFA, CH₂Cl₂, anisol, 0 °C to rt, 3 h; (h) EDC-HCl, HOBT, DIPEA, DMF, THF, 2 mM, rt, 13 h, 21% in 2 steps.

Acknowledgments

We thank Yuko Aoki and Shige Nagahashi for their helpful suggestions and comments. We also thank Masami Kohchi, Takehiro Okada, Yoshiaki Isshiki, Toshihiko Fujii, Kiyooki Sakata, Young-Jin Na, Sung-Jin Kim, Dong-Oh Yoon, Young-Jin Kwon, Azusa Hoshino, Shin-ichi Arai and all people who contributed to this work.

Supplementary data

Supplementary data associated with this article can be found, in the online version, at [doi:10.1016/j.bmcl.2011.11.100](https://doi.org/10.1016/j.bmcl.2011.11.100).

References and notes

- Richter, K.; Buchner, J. *J. Cell Physiol.* **2001**, *188*, 281.
- Maloney, A.; Workman, P. *Expert Opin. Biol. Ther.* **2002**, *2*, 3.
- Dai, C.; Whitesell, L. *Future Oncol.* **2005**, *1*, 529.
- Neckers, L. *J. Biosci.* **2007**, *32*, 517.
- Stebbins, C. E.; Russo, A. A.; Schneider, C.; Rosen, N.; Hartl, F. U.; Pavletich, N. P. *Cell* **1997**, *89*, 239.
- Schulte, T. W.; Akinaga, S.; Murakata, T.; Agatsuma, T.; Sugimoto, S.; Nakano, H.; Lee, Y. S.; Simen, B. B.; Argon, Y.; Felts, S.; Toft, D. O.; Neckers, L. M.; Sharma, S. V. *Mol. Endocrinol.* **1999**, *13*, 1435.
- Kamal, A.; Thao, L.; Sensintaffar, J.; Zhang, L.; Boehm, M. F.; Fritz, L. C.; Burrows, F. J. *Nature* **2003**, *425*, 407.
- Chiosis, G.; Neckers, L. A. C. *S. Chem. Biol.* **2006**, *1*, 279.
- Panaretou, B.; Siligardi, G.; Meyer, P.; Maloney, A.; Sullivan, J. K.; Singh, S.; Millson, S. H.; Clarke, P. A.; Naaby-Hansen, S.; Stein, R.; Cramer, R.; Mollapour, M.; Workman, P.; Piper, P. W.; Pearl, L. H.; Prodromou, C. *Mol. Cell* **2002**, *10*, 1307.
- Siligardi, G.; Panaretou, B.; Meyer, P.; Singh, S.; Woolfson, D. N.; Piper, P. W.; Pearl, L. H.; Prodromou, C. *J. Biol. Chem.* **2002**, *277*, 20151.
- Schulte, T. W.; Neckers, L. M. *Cancer Chemother. Pharmacol.* **1998**, *42*, 273.
- Egorin, M. J.; Lagattuta, T. F.; Hamburger, D. R.; Covey, J. M.; White, K. D.; Musser, S. M.; Eiseman, J. L. *Cancer Chemother. Pharmacol.* **2002**, *49*, 7.
- Lundgren, K.; Zhang, H.; Brekken, J.; Huser, N.; Powell, R. E.; Timple, N.; Busch, D. J.; Neely, L.; Sensintaffar, J. L.; Yang, Y. C.; McKenzie, A.; Friedman, J.; Scannevin, R.; Kamal, A.; Hong, K.; Kasibhatla, S. R.; Boehm, M. F.; Burrows, F. J. *Mol. Cancer Ther.* **2009**, *8*, 921.
- Brough, P. A.; Aherne, W.; Barril, X.; Borgognoni, J.; Boxall, K.; Cansfield, J. E.; Cheung, K. M.; Collins, I.; Davies, N. G.; Drysdale, M. J.; Dymock, B.; Eccles, S. A.; Finch, H.; Fink, A.; Hayes, A.; Howes, R.; Hubbard, R. E.; James, K.; Jordan, A. M.; Lockie, A.; Martins, V.; Massey, A.; Matthews, T. P.; McDonald, E.; Northfield, C. J.; Pearl, L. H.; Prodromou, C.; Ray, S.; Raynaud, F. I.; Roughley, S. D.; Sharp, S. Y.; Surgenor, A.; Walmsley, D. L.; Webb, P.; Wood, M.; Workman, P.; Wright, L. J. *J. Med. Chem.* **2008**, *51*, 196.
- Woodhead, A. J.; Angove, H.; Carr, M. G.; Chessari, G.; Congreve, M.; Coyle, J. E.; Cosme, J.; Graham, B.; Day, P. J.; Downham, R.; Fazal, L.; Feltell, R.; Figueroa, E.; Frederickson, M.; Lewis, J.; McMennamin, R.; Murray, C. W.; O'Brien, M. A.; Parra, L.; Patel, S.; Phillips, T.; Rees, D. C.; Rich, S.; Smith, D. M.; Trewartha, G.; Vinkovic, M.; Williams, B.; Woolford, A. J. *J. Med. Chem.* **2010**, *53*, 5956.
- Miura, T.; Fukami, T. A.; Hasegawa, K.; Ono, N.; Suda, A.; Shindo, H.; Yoon, D. O.; Kim, S. J.; Na, Y. J.; Aoki, Y.; Shimma, N.; Tsukuda, T.; Shiratori, Y. *Bioorg. Med. Chem. Lett.* **2011**, *21*, 5778.
- MOE (Molecular Operating Environment), Chemical Computing Group Inc., <http://www.chemcomp.com/software.htm>.
- Marsault, E.; Peterson, M. L. *J. Med. Chem.* **2011**, *54*, 1961.
- Veber, D. F.; Johnson, S. R.; Cheng, H. Y.; Smith, B. R.; Ward, K. W.; Kopple, K. D. *J. Med. Chem.* **2002**, *45*, 2615.
- Bissant, C.; Kuhn, B.; Stahl, M. *J. Med. Chem.* **2010**, *53*, 5061.
- TPSA, Daylight Chemical Information Systems, Inc., <http://www.daylight.com>.
- Ertl, P.; Rohde, B.; Selzer, P. *J. Med. Chem.* **2000**, *43*, 3714.
- Ono, N.; Yamazaki, T.; Nakanishi, Y.; Fujii, T.; Sakata, K.; Tachibana, Y.; Suda, A.; Hada, K.; Miura, T.; Sato, S.; Saitoh, R.; Nakano, K.; Tsukuda, T.; Mio, T.; Ishii, N.; Kondoh, O.; Aoki, Y. *Cancer Sci.* **2011**, in press, doi:10.1111/j.1349-7006.2011.02144.x.